01 Jan 2008

Simulation of the Evolution of the Nanostructure of Crosslinked Silica-Aerogels under Compression

Hongbing Lu

Boshen Fu

Nitin Daphalapurkar

Jay Hanan

et. al. For a complete list of authors, see https://scholarsmine.mst.edu/chem_facwork/2381

SIMULATION OF THE EVOLUTION OF THE NANOSTRUCTURE OF CROSSLINKED SILICA-AEROGELS UNDER COMPRESSION

Hongbing Lu[a], *Boshen Fu*[a], *Nitin Daphalapurkar*[a], *Jay Hanan*[a], *Chariklia Sotiriou-Leventis*[b] *and Nicholas Leventis*[b]

[a]School of Mechanical and Aerospace Engineering, Oklahoma State University, Stillwater, OK 74078
[b]Department of Chemistry, Missouri University of Science and Technology, Rolla, MO 65409

E-mails: hongbing.lu@oksate.edu, leventis@mst.edu; cslevent@mst.edu

Introduction

Silica-aerogels are ultra-low-density assemblies of silica nanoparticles, and possess superior acoustic, specific energy absorption and thermal insulation properties. A new class of aerogels encapsulated with polymer is classified as crosslinked silica-aerogels. Manufacturing of such crosslinked silica-aerogel structures, depending on the type and shape of the nanoparticles, the polymer cross-linker and the chemistry in use, yields structures with vastly different morphologies and a wide range of mechanical behavior. With this, it has become necessary to understand the nanostructure / macroscopic properties relationship. Modeling of the aerogel material properties from mesoscale and up approach is needed, which is not considered by the current phenomenological models based on continuum material assumption. Most of the existing simulation methodologies face difficulties mainly due to complex nanostructures, large distortions, and extensive contact. A relatively new numerical method called Material Point Method (MPM) can circumvent these problems. For example, MPM has been used effectively in modeling the microstructural evolution of the bulk metallic glass foam with 70% porosity,[1] where 3D X-Ray microtomography was used first to obtain the representative volume element (RVE) of the closed-cell foam . Due to the particle description of matter, MPM is a very suitable for silica-aerogel simulations. In this regard, an approach based on X-Ray nano-computed tomography (n-CT) will be used to model cross-linked aerogel mesostructure. The voxel information from the 3D tomography will be used to generate material points in MPM. The parallel version (using Structured Adaptive Mesh Refinement Application Infrastructure) of MPM code will be used to simulate the response of the model under compression.

In this paper, the MPM is used to model a crosslinked templated silica-aerogel (X-MP4-T045) in compression, and the simulation results are compared with the compressive stress-strain curve obtained experimentally. This work will focus on the deformation mechanisms in crosslinked templated silica-aerogel such as the elastic buckling, compaction and densification, as well as the dependence of mechanical properties on the porosity effect for this crosslinked templated silica-aerogel.

Experimental

Materials. The material simulated was what is referred to as X-MP4-T045. [2,3] Using Nakanishi's notation, "M" stands for Mesoporous, "P4" refers to the specified amount of the templating agent (Pluronic P123) used in the standard formulation and "T045" refers to the specific amount of the swelling agent (trimethylbenzene) used in the standard recipe. That formulation yields macroporous structures consisting of micron-sized worm-like objects, which in turn are perforated with mesoporous tubes. "X" signifies that the MP4-T045 microstructure has been crosslinked with a polymer.[4]

Nano-Computerized Tomography (n-CT). To generate the nanostructure model for the MPM simulation, nanostructure was obtained using a n-CT. During each scanning step, X-ray with an initial intensity I_0 passes through a specimen. As the sample absorbs part of this energy, the incident intensity of the X-ray is attenuated to I. A scintillator converts the X-ray to visible light, which is acquired by a CCD camera X-ray images are taken at quarter degree increments from 0º to 180º and appear as radiographs. The radiographs are combined to reconstruct a series of two-dimensional (2D) images representing the local density of the material. The n-CT tomographic image was used to generate the three-dimensional MPM model, as shown in Figure 1 for MPM simulation.

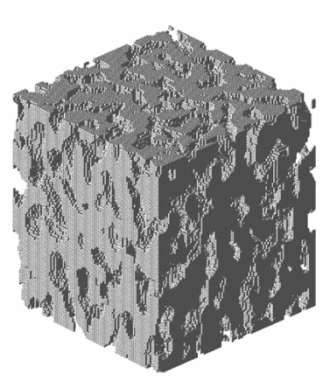

Figure 1. 3D discretized MPM model for a crosslinked template silica-aerogel (X-MP4-T045) by converting the grayscale n-CT information into material points.

Results and Discussion

Material Point Method (MPM). The material point method was used to model the crosslinked template silica-aerogel under compression, it is introduced briefly. MPM was evolved from Particle-in-Cell (PIC) method,[5] and formulated for simulation of solid mechanics problem by Sulsky *et al.*[6] in 1995. Further developments have been made since then.[7-12] In MPM, the material continuum is discretized into finite material areas in 2D (or volumes for the 3D case). Each material point is assigned a mass consistent with the material density and volume of the point, and all of variables used in the simulation, such as position, velocity, acceleration, stress, and strain. In this work, we use a C^1 continuous weighting function as given by Bardenhagen *et al.*[7] The equation of motion is solved at each node to update the nodal momentum, acceleration, and velocity. These updated nodal variables are then interpolated to the material points to update the particle position, velocity, stress, and strain. In this paper, we consider the linear elastic, isotropic material properties for the secondary particles in the crosslinked aerogels. The effective modulus determined from silica secondary nanoparticles and the polymer coating was used in simulation.

Modeling of crosslinked template silica-aerogel. The resolution of the original images was reduced (reduction of 2×2×2 voxels to 1 voxel) to simulate a larger piece of aerogel. Each material point length represents 480 nm. Within the cell-walls the material was assumed to be uniform, with the consideration of the effective properties determined from silica secondary particle and polymer coating. For conducting simulations at different porosities, we found that there is a linear relation between the cut-off grayscale of the images and the porosity of the sample. The skeletal density of X-MP4-T045 with bulk density of 0.663 g/cm^3 is 1.320 g/cm^3. The skeletal density of the silica underneath the polymer is 1.935 g/cm^3. The Poisson's ratio is assumed to be 0.3. The diameter of the secondary particles for the X-MP4-T045 is about 1 μm, and the polymer weight percentage is about 70%.[3] Based on these properties we calculated the effective Young's modulus of the cell walls to be 3.9 GPa. In compression simulation of crosslinked templated silica-aerogels using MPM, the bottom the model was fixed using displacement boundary conditions. All side walls are confined. Frictionless contact was assumed when the material points move along the side walls. Meanwhile, the constraint applied on all faces of the cube, leads to material points to move only inside the cube. On the top of the model, another relatively rigid plate was added and the velocity boundary condition was applied on it, simulating the compression of the testing machine. In such a dynamic problem the force is initially applied on the top, but its effect cannot reach the bottom side of the model instantaneously. The compressive stress wave will have to travel to the bottom and then be reflected back; it usually takes three to five round-trip transits to allow the force at the top to be nearly equal to the force at the bottom of the sample.

Simulations. From the n-CT information, the average pore size of X-MP4-T045 is about 6~7 μm, and the wall thickness of the nanostructure is about 2~3 μm. To determine the appropriate RVE size, we simulated a cube with a side length equal four times of the pore size (4× pore size), and then we increased the side length incrementally, up to 8× of the pore size. The results converge when 8× pore size (52.8 μm) was used as the side length of the cubic RVE. For this RVE, the porosity converges to 50%, which is the actual

porosity of the material. Figure 2 shows the stress as a function of strain from simulations and experiment. With the silica-aerogel compressed, the stress increases linearly with strain at small deformations. The dynamic equilibrium condition was satisfied after the stress wave travels by a few round trips. The simulation results show that the material yields at about 4% compressive strain, in agreement with the experimental data. The stress-stain curve of the simulation matches almost exactly the experiment results at small deformations, up to 5%. Figure 3 shows the deformed states, and Figure 4 shows the section views of the same simulation. In general the pores are crushed in deformation, and the deformation occurs throughout the entire model. This phenomenon is different from that of a plastic foam, in which compaction occurs as weak planes induce propagation of compaction waves which leads to highly localized deformations.

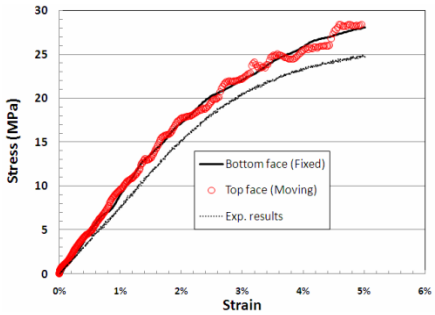

Figure 2. Compressive stress-strain curves from the MPM simulation showing the dynamic equilibrium.

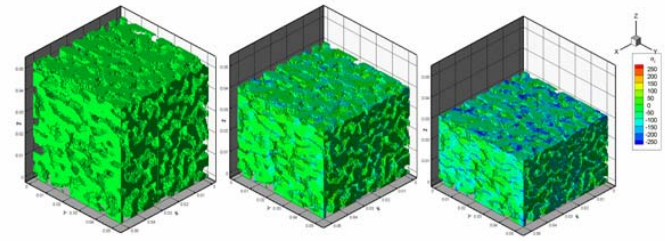

Figure 3. 3D views of foam RVE in compression from MPM simulation.

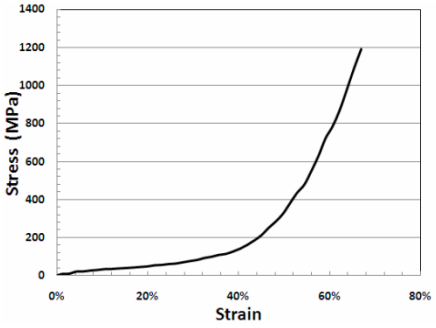

Figure 4. Compression of stress strain curve obtained from numerical simulation using MPM. The stress strain relation at small strains is shown in Figure 2.

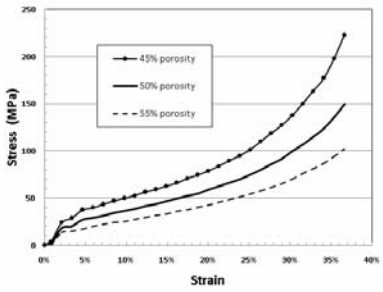

Figure 5. Compressive stress-strain curve for model with different porosity obtained from numerical simulation using MPM. The curves follow a cubic power relation with density.

Figure 4 shows the stress-strain response under compression for 50% porosity crosslinked templated silica-aerogel model. The curve shows the typical features of a porous material, with an initial linear elastic region, followed by compaction and a final densification region. The confined boundary condition applied on the four sides of the model might have induced stress that is higher than the experimental value. Figure 5 shows the stress-strain curves for the models with three porosity values, 45%, 50% and 55%. The simulation results indicate that the stress-strain relation follows nearly a power law relation with density, consistent with the theory of Gibson *et al*[13] appropriate for porous materials with relatively high porosity.

Conclusions

The material point method has been used to simulate the compression of the crosslinked templated silica-aerogel using the nanostructure determined from nano-CT. This method can handle the large deformation (even above 80%) within the densification region. The stress-strain response was for the templated aerogels using the elastic-plastic material constitutive model. The stress-strain curve from the MPM simulation indicates that the dynamic equilibrium has been established at low strains within the elastic region. The stress-strain relation matches with the experimental results in the elastic region. The simulation can capture the characteristics of a typical stress-strain relation of the templated crosslinked silica aerogels, namely elastic, compaction, and densification regions. Nearly uniform deformation was observed in compression, in contrast to propagation of compaction waves as observed in plastic foams. The effect of porosity was simulated for three values of the porosity. Results show that the stress-strain relation follows a cubic power law relation with mass density for porosity ranging from 45% to 55%. The results in this work show the potential of using MPM to simulate the nanostructure property relationship of crosslinked silica aerogels.

Acknowledgements. We thank the NSF under CMMI-0653919 & CMMI-0653970 for financial support.

References

(1) Daphalapurkar, N., Hanan, J. Phelps, N., Bale, H., Lu, H. *Mech. Adv. Mater. & Struc*., **2008**, in press
(2) Nakanishi, K., J. Porous Mater. **1997**, 4, 67
(3) Leventis, N. Mulik, S., Wang, X., Dass, A. Patil, V., Sotiriou-Leventis, C. Lu, H., *J. Non-cryst. Solids*, **2008**, 354, 632-644
(4) Leventis,N. Mulik, S. Wang, X. Dass, A. Sotiriou-Leventis, C. Lu, H., *J. Am. Chem. Soc.*, **2007**, 129, 10660
(5) Harlow, F., *Meth. Comp. Phys*., **1963**, 3, 319
(6) Sulsky, D. Zhou, S., Schreyer, H., *Comput. Phys. Commun.* **1995**, 3, 236
(7) Bardenhagen, S. Kober, E., *Comput. Mod. Engng. Sc.*, **2000**, 1, 11
(8) Tan, H. Nairn, *J. Comput. Method Appl. M.* **2002**, 191 2095-2109
(9) Daphalapurkar, N., Lu, H., Coker, D., Komanduri, R., *Int. J. Fract*., **2006**, 143, 79
(10) Ma, J. Lu, H., Komanduri, R., *Comput. Mod. Engng. Sc.*, **2006**, 12, 213
(11) Ma, J. Lu, H., Wang, B., Roy, S., Hornung, R., Wissink, A., Komanduri, R., *Comput. Mod. Engng. Sc.*, **2005**, 8, 135
(12) Ma, J. Lu, H., Wang, B., Roy, S., Hornung, R., Wissink, A., Komanduri, R., *Comput. Mod. Engng. Sc.*, **2006**, 14, 101
(13) Gibson, L., Ashby, M., *Cellular Solids, 2nd Ed.* , **1997**